


Initial evaluation of PET/CT with ^{18}F -FSU-880 targeting prostate-specific membrane antigen in prostate cancer patients

Tsuneo Saga¹  | Yuji Nakamoto¹ | Takayoshi Ishimori¹ | Takahiro Inoue² | Yoichi Shimizu¹ | Hiroyuki Kimura^{3,4} | Shusuke Akamatsu² | Takayuki Goto² | Hiroyuki Watanabe³ | Kosuke Kitaguchi¹ | Masao Watanabe¹ | Masahiro Ono³ | Hideo Saji³ | Osamu Ogawa² | Kaori Togashi¹

¹Department of Diagnostic Imaging and Nuclear Medicine, Graduate School of Medicine, Kyoto University, Kyoto, Japan

²Department of Urology, Graduate School of Medicine, Kyoto University, Kyoto, Japan

³Department of Patho-Functional Bioanalysis, Graduate School of Pharmaceutical Sciences, Kyoto University, Kyoto, Japan

⁴Department of Analytical and Bioinorganic Chemistry, Kyoto Pharmaceutical University, Kyoto, Japan

Correspondence

Tsuneo Saga, Department of Diagnostic Imaging and Nuclear Medicine, Graduate School of Medicine, Kyoto University, Kyoto, Japan.

Email: saga@kuhp.kyoto-u.ac.jp

Funding information

Japan Agency for Medical Research and Development, Grant/Award Number: 17ck01064149h003, 18ck0106426h001

This first-in-man study was carried out to evaluate the safety, whole-body distribution, dose estimation, and lesion accumulation of ^{18}F -FSU-880, a newly developed probe targeting prostate-specific membrane antigen. Six prostate cancer patients with known metastatic lesions underwent serial whole-body PET/computed tomography (CT) with ^{18}F -FSU-880. Blood and urine were analyzed before and after PET/CT. Accumulation of ^{18}F -FSU-880 in organs and metastatic lesions in serial PET images were evaluated by measuring the standardized uptake values. From the biodistribution data, the organ doses and whole-body effective dose were calculated using OLINDA/EXM software was developed by Dr. Michael Stabin of Vanderbilt University, Nashville, Tennessee, USA. ^{18}F -FSU-880 PET/CT could be carried out without significant adverse effects. High physiological uptake was observed in the salivary/lachrymal glands and kidneys. The effective dose was calculated to be 0.921×10^{-2} mSv/MBq. Known metastatic lesions were clearly visualized with high image contrast that increased with time, except in 1 patient, whose bone metastases were well-controlled and inactive. The PET/CT with ^{18}F -FSU-880 could be carried out safely and could clearly visualize active metastatic lesions. The present results warrant further clinical studies with a larger number of cases to verify the clinical utility of ^{18}F -FSU-880 PET/CT in the management of prostate cancer patients.

KEYWORDS

dosimetry, fluorine-18, positron emission tomography/computed tomography, prostate cancer, prostate-specific membrane antigen

1 | INTRODUCTION

Prostate cancer is one of the most common malignancies in men and leads to substantial morbidity and mortality.¹ According to the projected cancer statistics of Japan, 2018, reported from the

National Cancer Center, Japan, prostate cancer ranks fourth in the projected cancer incidence in men, and sixth in the projected cancer death in men (https://ganjoho.jp/en/public/statistics/short_pred.html).² As the prognosis of patients with localized prostate cancer is mostly favorable, therapeutic strategies should be

UMIN Clinical Trials Registry: UMIN000029343

This is an open access article under the terms of the Creative Commons Attribution-NonCommercial License, which permits use, distribution and reproduction in any medium, provided the original work is properly cited and is not used for commercial purposes.

© 2018 The Authors. *Cancer Science* published by John Wiley & Sons Australia, Ltd on behalf of Japanese Cancer Association.

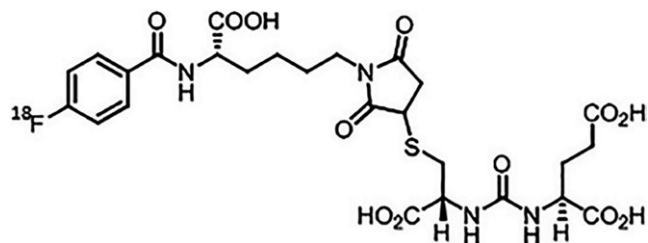


FIGURE 1 Chemical structure of ^{18}F -FSU-880

adapted to the stage and grade of the individual prostate cancer case.³ Medical imaging is expected to play an important role in the characterization of prostate cancer for personalized medicine.⁴

Recently, prostate-specific membrane antigen (PSMA) has received attention as a target of imaging and therapy for prostate cancer.⁵ Prostate-specific membrane antigen is a cell-surface enzyme also known as glutamate carboxypeptidase II or folate hydrolase.⁶ It is overexpressed on most prostate cancer cells and its expression increases in higher grade cancers and in metastatic and recurrent cancers.^{7,8} Furthermore, the level of PSMA expression is correlated with prognosis.⁹ Although PSMA is physiologically expressed in normal tissues such as the proximal renal tubules, salivary/lachrymal glands, and small intestine, and on neo-vasculatures of some cancers such as renal cancer,¹⁰ normal prostate tissue expresses only a small amount in the apical epithelium of the secretory ducts.⁸ Therefore, PSMA is regarded as an optimal imaging and therapy target in prostate cancer.

Although PSMA-targeted imaging in prostate cancer was initially carried out using radiolabeled anti-PSMA Abs, the use of radiolabeled small molecular weight PSMA inhibitors is becoming more popular.^{11,12} The clinical utility of PET/computed tomography (CT) using ^{68}Ga -labeled PSMA inhibitors, such as ^{68}Ga -PSMA-11, which is the most widely used inhibitor, has been reported in many papers.^{13,14} Recently, ^{18}F -labeled PSMA inhibitors have also been developed and used clinically.^{15,16} Furthermore, PSMA inhibitors labeled with the β -emitter, ^{177}Lu , and the α -emitter, ^{225}Ac , have been introduced for PSMA-targeted radioligand therapy and have yielded promising therapeutic results.^{12,17,18}

Despite the worldwide application of PSMA-targeted ligands in the imaging and treatment of prostate cancer, prostate cancer patients in Japan are unable to benefit from these PSMA-targeted probes. Recently, a small molecule PET probe based on a PSMA-inhibitor labeled with ^{18}F has been developed at our institution.¹⁹ Preclinical studies indicated that this PET probe, named ^{18}F -FSU-880, possesses a high binding affinity for PSMA and shows a favorable pharmacokinetic profile with high accumulation in PSMA-expressing tumors.¹⁹ The present first-in-man study was undertaken to evaluate the safety, whole-body distribution, dose estimation, and lesion accumulation of ^{18}F -FSU-880.

2 | MATERIALS AND METHODS

2.1 | Inclusion/exclusion criteria for patients and study protocol

Patients with prostate cancer were eligible for enrollment if they were 20-85 years old with known metastatic lesions. Patients were

excluded if their general condition was very poor or if they had severe renal dysfunction that might alter the biodistribution of ^{18}F -FSU-880 (estimated glomerular filtration rate of $<30\text{ mL}/1.73\text{ m}^2$).

The study protocol was approved by the ethical committee of Kyoto University Graduate School of Medicine and Kyoto University Hospital (Kyoto, Japan; approval no. C1327), and was registered at the UMIN Clinical Trials Registry as UMIN000029343. The study was carried out in accordance with the ethical standards of the Declaration of Helsinki (as revised in Fortaleza, Brazil, October 2013). All patients provided written informed consent for participation in the study.

Prior to ^{18}F -FSU-880 PET/CT and within 10 days of ^{18}F -FSU-880 PET/CT, blood and urine samples were collected from the patients and analyzed for safety evaluation.

2.2 | ^{18}F -FSU-880 PET/CT

^{18}F -FSU-880 (Figure 1) was prepared on a COSMIC-Compact 24XX automated synthesis module (NMP Business Support Company, Chiba, Japan), following previously published methods,¹⁹ and was filter-sterilized.

The PET/CT studies were carried out using an integrated PET/CT scanner (Discovery IQ; GE Healthcare, Waukesha, WI, USA) with a bismuth germanate scintillator arranged in five rings and a 16-detector-row CT scanner. Patients fasted for >4 hours before their study. After evaluating the vital signs of the patients (blood pressure, heart rate, and respiration rate), low-dose CT was carried out for attenuation correction and for image fusion without oral/i.v. contrast. ^{18}F -FSU-880 (115.4-180.3 MBq) was then slowly given i.v. Whole-body emission data acquisition commenced 30 seconds after injection of ^{18}F -FSU-880 and was repeated 4 times. Emission data were acquired in 3D mode starting from the femur to the skull. The first and second scans (PET 1 and PET 2, respectively) consisted of 1 minute/frame \times 6 frames, and the third and fourth scans (PET 3 and PET 4, respectively) consisted of 2 minute/frame \times 6 frames. After PET 4, patients were asked to void for the radioactivity measurement of the urine. The final scan (PET 5) was undertaken 2 hours after administration of ^{18}F -FSU-880. The vital signs were evaluated again after PET 5.

During PET/CT, blood samples were collected four times (immediately after starting PET 1, and at the end of PET 2, PET 4, and PET 5), and the radioactivity of the whole blood and plasma was evaluated.

2.3 | Image analysis

Images of the whole body from the skull to the femur were reconstructed using an ordered subset expectation maximization algorithm (subsets, 14; iteration, 2) with CT-attenuation correction. Point spread function correction was also carried out.

The PET/CT images were visually reviewed on a workstation (Advantage Workstation 4.6; GE Healthcare) by 2 board-certified nuclear medicine physicians (TS and YN), who were not blinded to

TABLE 1 Characteristics of 6 patients with prostate cancer

Case	At initial diagnosis				At ¹⁸ F-FSU-880 PET/CT				
	Age (y)	Clinical stage	Gleason score	PSA (ng/mL)	Initial treatment	CRPC	PSA (ng/mL)	Known lesion site	Treatment
1	74	cT4N1M1	4 + 4 = 8	206.00	CAB	Yes	8.72	Bone	No therapy
2	74	cT3aN0M0	4 + 4 = 8	13.20	CAB + IMRT	No	2.61	LN	No therapy
3	71	cT3aN0M1	4 + 5 = 9	26.90	CAB	Yes	7.83	Bone	Enzalutamide
4	55	cT2cN1M1	4 + 3 = 7	280.00	CAB	Yes	5.39	Bone	Abiraterone acetate
5	80	cTxNxM1	4 + 5 = 9	487.00	CAB	Yes	0.01	Bone	²²³ Ra-chloride
6	77	cT3aN0M0	4 + 3 = 7	11.12	CAB + IMRT	Yes	1.70	Bone	Abiraterone acetate

CAB, combined androgen blockade therapy (gonadotropin-releasing hormone antagonist/luteinizing hormone-releasing hormone analog + antiandrogen); CRPC, castration-resistant prostate cancer; CT, computed tomography; IMRT, intensity-modulated radiation therapy; LN, lymph node; PSA, prostate-specific antigen.

the clinical and imaging information of the patients. In PET 1 images, volumes of interest (VOIs) were generated on various normal organs and a blood pool (left ventricle) by referring to the corresponding CT images. Volumes of interest were reproduced on PET 2 to PET 5 images and the average standardized uptake values (SUVmean) were obtained. In PET 5 images, focal increased uptakes compared to that in the surrounding normal tissue or blood pool, excluding apparent physiological uptakes, were regarded as recurrent/metastatic lesions and VOIs were placed where the maximal SUVs (SUVmax) were obtained. The VOIs were reproduced on the PET 1 to PET 4 images for SUV evaluation. Tumor-to-blood ratios (TBRs) were also calculated by dividing the lesion SUVmax by the SUVmean of blood pool (heart content) of the corresponding PET series.

2.4 | Radioactivity in blood and urine

Collected blood was divided into whole blood and plasma samples. Both samples were weighed and counted for radioactivity using a well-type γ -counter. Urine samples were measured for volume and the radioactivity was counted. All count data were decay-corrected and adjusted at the time of probe administration.

2.5 | Radiation dosimetry

The Medical Internal Radiation Dose S values as implemented in the software OLINDA/EXM version 1.1 were used for radiation dosimetry. The SUVmeans in the source organs at various time points were converted to percentages of the injected dose per mL (%ID/mL), which were multiplied by the volume of each organ to generate percentages of the injected dose per organ at each time point. Time-activity curves of each source organ were then generated and time-integrated activity coefficients (residence times) were obtained. From these values, the organ absorbed doses and effective doses of each patient were calculated using OLINDA/EXM version 1.1.

3 | RESULTS

3.1 | Demographics

Six prostate cancer patients with known metastatic lesions were included in the present study (Table 1). The serum prostate-specific antigen (PSA) values at the time of PET/CT ranged from 0.01 to 8.72 ng/mL. Five patients were known to have bone metastases by CT and/or bone scintigraphy and the remaining 1 patient had lymph node (LN) metastasis detected by CT.

3.2 | Safety

Administration of ¹⁸F-FSU-880 was carried out safely without the occurrence of any acute adverse events. No significant change in vital signs was observed after PET/CT compared to those obtained before PET/CT. Blood and urine analyses were undertaken before

and 5-8 days after PET/CT. Changes in blood/urine data (normal range before PET/CT changed to abnormal range after PET/CT) were observed in 4 out of 6 patients. In case 1, the blood urea nitrogen level (normal range, 8.0-22.0 mg/dL) increased from 20.9 to 23.5 mg/dL, although the serum creatinine levels remained within the normal range. In case 2, the lactate dehydrogenase (LDH) level (normal range, 121-245 U/L) increased from 227 to 263 U/L. In case 3, the blood urea nitrogen level increased from 22.0 to 24.7, but the serum creatinine levels remained within the normal range. In case 5, the white blood cell count (normal range, $39-98 \times 10^2/\mu\text{L}$) decreased from 49 to $37 \times 10^2/\mu\text{L}$, and the total bilirubin level (normal range, 0.2-1.2 mg/dL) increased from 1.0 to 1.4 mg/dL. In the remaining 2 cases, cases 4 and 6, no changes in blood/urine data were observed.

In order to rule out the possibility of late phase adverse effects of ^{18}F -FSU-880, clinical conditions of the 6 cases were followed up after PET/CT (follow-up periods ranged from 5 to 8 months). Case 1 developed antineutrophil cytoplasmic Ab (ANCA)-associated vasculitis and received high-dose steroid treatment and recovered. During this period, his serum hepatobiliary enzyme levels (glutamic oxaloacetic transaminase, glutamic pyruvic transaminase, LDH, alkaline phosphatase [ALP], and γ -glutamyl transpeptidase [γ -GTP]) were slightly elevated, which were recovering after tapering the dose of steroid. In the remaining 5 cases, no clinical event that required medical intervention was observed. Case 2 showed fluctuation of

his serum levels of glutamic oxaloacetic transaminase, LDH, ALP, γ -GTP, and leucine aminopeptidase, but the deviation from normal range was minimal. In case 3, who showed progressive worsening of his bone metastases and the appearance of liver and adrenal metastases, his serum levels of LDH and ALP increased. Case 4 showed fluctuation of laboratory data (ALP and γ -GTP), but there was little deviation from the normal range. In case 5, his serum level of γ -GTP showed elevated values at the last follow-up (122 U/L; normal range, 9-54 U/L) with otherwise no abnormal data. Case 6 indicated no abnormality in his laboratory data.

3.3 | Whole-body distribution and dose estimation

Whole-body maximal intensity projection images of PET 1 to PET 5 in case 6 are illustrated in Figure 2A as a representative of the 6 cases. High uptake of ^{18}F -FSU-880 was observed in the known bone metastasis in the upper thoracic vertebra, which was already evident in PET 1 and became clearer with time. With regard to physiological uptake, high uptake was observed in the kidneys, followed by the salivary and lachrymal glands, and moderate uptake was noted in the liver and spleen. Urinary bladder uptake increased with time, indicating excretion of ^{18}F -FSU-880 through the kidneys. The time course of the SUVmean in various organs (brain, parotid gland, liver, spleen, kidney, and heart content) in case 6 is presented in Figure 2B.

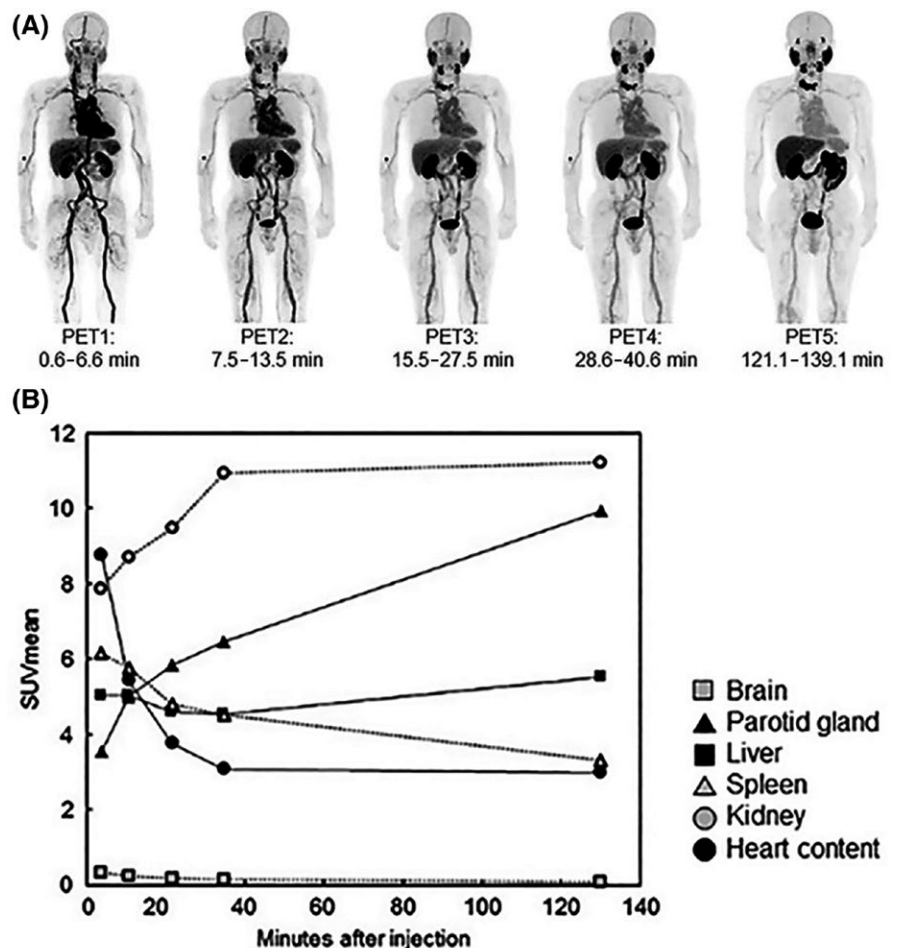


FIGURE 2 Whole-body distribution of ^{18}F -FSU-880 in case 6, a prostate cancer patient with known metastatic lesions. A, Maximum intensity projections of 5 serially performed ^{18}F -FSU-880 PET. B, Time course of the average standardized uptake value (SUVmean) in various normal organs and the blood pool

Radioactivity counting in the whole blood and plasma indicated that >88.5% (range, 88.5%-98.3%) radioactivity was detected in the plasma fraction. The change in blood activity derived from the VOI/SUV analysis of the heart content was mostly comparable with that derived from γ -counting of whole blood activity (data not shown).

Urine collected between PET 4 and PET 5 was assessed for radioactivity, and the results indicated that 8.0%-13.2% of total radioactivity was excreted into the urine.

Dosimetry analyses were applied using the PET SUV data and OLINDA/EXM software. The results are summarized in Table 2, indicating the mean \pm SD of the 6 cases. The highest absorbed dose was observed in the kidney (5.435×10^{-2} mSv/MBq) followed by the liver (2.380×10^{-2} mSv/MBq), spleen (1.910×10^{-2} mSv/MBq), and urinary bladder wall (1.878×10^{-2} mSv/MBq). The effective dose was determined to be 0.921×10^{-2} mSv/MBq, indicating that the whole-body dose was approximately 1.7 mSv after giving 185 MBq ^{18}F -FSU-880.

TABLE 2 Dosimetry results of ^{18}F -FSU-880, a newly developed probe targeting prostate-specific membrane antigen, in 6 prostate cancer patients with known metastatic lesions

Organ (mSv/MBq)	Mean ($\times 10^{-2}$)	SD ($\times 10^{-2}$)
Adrenals	0.838	0.105
Brain	0.157	0.021
Breasts	0.409	0.052
Gallbladder wall	0.948	0.090
LLI wall	0.970	0.135
Small intestine	1.307	0.266
Stomach wall	0.837	0.092
ULI wall	0.728	0.024
Heart wall	1.843	0.272
Kidneys	5.435	1.690
Liver	2.380	0.280
Lungs	0.571	0.075
Muscle	0.488	0.055
Pancreas	1.272	0.257
Red marrow	0.635	0.073
Osteogenic cells	0.763	0.095
Skin	0.359	0.046
Spleen	1.910	0.509
Testes	0.436	0.049
Thymus	0.536	0.069
Thyroid	0.743	0.097
Urinary bladder wall	1.878	0.476
Total body	0.581	0.061
Effective dose (mSv/MBq)	0.921	0.080

LLI, lower large intestine; Mean, average of 6 patients; SD, standard deviation of 6 patients; ULI, upper large intestine.

3.4 | Lesion accumulation of ^{18}F -FSU-880

In 5 of 6 patients, known metastatic lesions were clearly visualized with SUVmax and image contrast (TBRs), which increased with time (Table 3). Larger lesions tended to show very high uptake of ^{18}F -FSU-880 and very high TBRs. Furthermore, additional abnormally increased uptakes were detected in 3 patients: recurrent lesion in the prostate was suspected in case 1 (Figure 3), additional LN metastasis in case 2, and multiple bone metastases in case 4 (Figure 4).

In case 5, the ^{18}F -FSU-880 uptake in known bone metastases remained low at all time points and did not increase with time, resulting in poor lesion-to-background contrast (TBR < 1 in all PET series).

4 | DISCUSSION

^{18}F -FSU-880 is a newly developed small molecule PET probe that targets PSMA.¹⁹ ^{18}F -FSU-880 has an asymmetric urea compound that acts as a binding moiety for PSMA, which is common among various radiolabeled PSMA-targeting probes (Figure 1). The structure-activity relationship was previously determined in an ^{123}I -labeled asymmetric urea compound and indicated that the aromatic ring and succinimidyl moiety are associated with high binding affinity.²⁰ From this finding, four ^{18}F -labeled probe candidates (^{18}F -8a, ^{18}F -8b, ^{18}F -10a, and ^{18}F -10b) with preserved aromatic ring and succinimidyl moiety were prepared using ^{18}F -N-succinimidyl 4-fluorobenzoate (^{18}F -SFB), a rapid and effective ^{18}F -labeling agent. Among them, ^{18}F -10a showed the highest binding affinity for PSMA ($K_i = 2.23$ nmol/L, which was determined by an inhibition assay with ^{125}I -N-[N-[(S)-1,3-dicarboxypropyl]carbamoyl]-S-3-iodo-L-Tyr) and accumulated in PSMA-expressing prostate cancer xenografts in mice at a level comparable to that of ^{18}F -DCFPyL.¹⁹ We therefore selected ^{18}F -10a for clinical evaluation and renamed it ^{18}F -FSU-880.

In the present first-in-man clinical study, administration of ^{18}F -FSU-880 could be carried out safely without the occurrence of significant adverse events. Although changes in blood analyses data were observed in 4 of 6 patients, the grade of the changes was minimal, and the values returned to within the normal range in all cases in the follow-up examinations without any clinical intervention. These changes could therefore be regarded to be within the range of physiological fluctuations and insignificant as adverse effects. In addition, no clinical events or data were observed suggesting late phase adverse effects. Case 1 suffered ACNA-associated vasculitis, which was likely to be independent to ^{18}F -FSU-880 PET/CT and his change in laboratory data could be attributed to the intensive steroid treatment. Increased LDH and ALP levels in case 3 were due to disease progression. The remaining 4 cases did not show significant changes in laboratory data suggestive of late phase adverse effects.

Repeated whole-body imaging illustrated the physiological distribution of ^{18}F -FSU-880, which was almost identical to that of other ^{68}Ga - and ^{18}F -labeled small molecule PSMA-targeting probes.^{15,16,21} This is quite reasonable as ^{18}F -FSU-880 has an asymmetric urea compound as a binding moiety that is common

TABLE 3 Change in the maximal standardized uptake value (SUV_{max}) of ¹⁸F-FSU-880, a newly developed probe targeting prostate-specific membrane antigen, and tumor-to-blood ratio (TBR) in lesions in 6 prostate cancer patients

Case	Lesion		PET 1	PET 2	PET 3	PET 4	PET 5
1	Prostate	SUV _{max}	3.51	5.60	6.16	6.74	13.34
		TBR	0.38	0.88	1.38	1.76	5.42
	Left pubic bone	SUV _{max}	2.80	4.98	6.18	6.78	13.25
		TBR	0.31	0.78	1.38	1.77	5.39
2	Left external iliac LN	SUV _{max}	8.50	7.69	10.04	13.30	24.27
		TBR	1.07	1.27	2.24	3.58	8.55
3	Right ischium	SUV _{max}	8.07	9.26	8.65	9.60	9.50
		TBR	0.72	1.15	1.37	1.89	3.74
4	L3	SUV _{max}	31.02	59.69	72.95	82.51	82.24
		TBR	3.00	7.81	13.84	17.52	24.62
	Th4	SUV _{max}	6.72	13.48	15.66	18.13	19.09
		TBR	0.65	1.77	2.97	3.85	5.72
5	L5	SUV _{max}	3.04	2.78	2.84	2.61	3.45
		TBR	0.26	0.32	0.51	0.55	0.96
6	Th1	SUV _{max}	7.26	11.15	15.63	18.57	37.09
		TBR	0.83	2.05	4.15	6.01	12.40
	Sternum	SUV _{max}	2.04	1.79	2.50	2.40	7.20
		TBR	0.23	0.33	0.66	0.78	2.41
	Left rib	SUV _{max}	1.96	2.49	3.45	3.53	5.17
		TBR	0.22	0.46	0.92	1.14	1.73

L, lumbar spine; LN, lymph node; Th, thoracic spine.

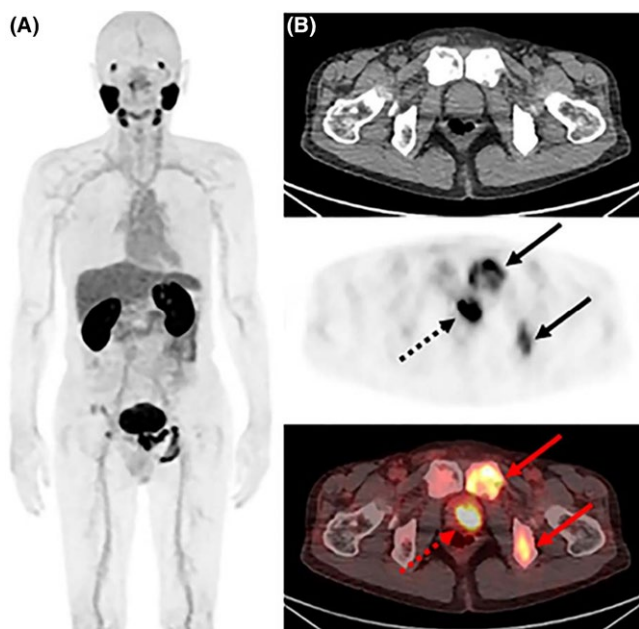


FIGURE 3 ¹⁸F-FSU-880 PET/computed tomography (CT) images of case 1, a prostate cancer patient with known metastatic lesions, obtained 2 h after administration. In addition to the increased uptake of ¹⁸F-FSU-880 in the known bone metastases (arrows), high uptake was also observed in the prostate gland, which was suggestive of local recurrence (dotted arrows). A, Maximum intensity projection image. B, Transaxial CT, PET, and PET/CT fusion images from top to bottom

among other small molecule PSMA inhibitors. The high uptake of ¹⁸F-FSU-880 observed in the kidneys and salivary and lachrymal glands might reflect physiological PSMA expression in these organs. However, the reported PSMA expression in the salivary glands was rather low compared to the observed high probe uptake, and radiolabeled anti-PSMA Ab did not show high salivary gland uptake,^{22,23} indicating that some additional mechanism related to the small molecular size should be considered.²⁴ Although a preclinical study had shown that ¹⁸F-FSU-880 is excreted exclusively from the kidneys,¹⁹ the amount of ¹⁸F-FSU-880 excreted into urine during the PET 4/PET 5 interval was relatively low (8.0%-13.2%), suggesting that more rigid hydration to accelerate diuresis would be beneficial in future studies to further reduce background activity and improve image contrast.

The organ dose calculation indicated that the kidneys received the highest dose, followed by the liver. However, renal dose is expected to reach approximately 10 mSv after administration of 185 MBq ¹⁸F-FSU-880, which is readily tolerable and regarded as an acceptable level. The total body effective dose of ¹⁸F-FSU-880 (0.921×10^{-2} mSv/MBq) was lower than that reported for other ¹⁸F-labeled PSMA probes (1.39 to 2.20×10^{-2} mSv/MBq),^{15,16,25} and was also acceptable.

In 5 of 6 patients, known metastatic lesions showed high uptake of ¹⁸F-FSU-880 and image contrast (tumor-to-blood ratio) increased with time, suggesting that ¹⁸F-FSU-880 PET/CT could sensitively depict recurrent/metastatic lesions. Furthermore, additional recurrent/metastatic lesions were suspected in 3 patients. As the major

aim of the present study was to evaluate the safety of ^{18}F -FSU-880 PET/CT, attempts to confirm all of these suspected lesions were not made. Further study should be undertaken to evaluate the clinical utility of ^{18}F -FSU-880 PET/CT in the detection of recurrent/metastatic lesions in a larger patient population.

In the remaining patient (case 5), known bone metastases showed very low uptake of ^{18}F -FSU-880 with a TBR < 1 at all time points. It is reported for ^{68}Ga - and ^{18}F -labeled PSMA probes that, in biochemical recurrence, patients with low serum PSA levels showed a low detection rate.²⁶ When PET/CT was carried out at very early stage with low PSA level, the lesion size was too small to be detected due to partial-volume effect. However, case 5 is not an early metastatic case but a case during treatment of metastases. This patient was treated with abiraterone acetate for multiple bone metastases in combination with radiation therapy to the lumbar spine. As the follow-up bone scintigraphy indicated that some of the bone metastases still showed increased uptake of the bone agent, he further received internal radiotherapy with ^{223}Ra -chloride. ^{18}F -FSU-880 PET/CT was performed during this ^{223}Ra -chloride treatment. The patient's serum PSA level was very low at the time of PET/CT, which remained very low thereafter (<0.02 ng/mL). Furthermore, bone scintigraphy undertaken 2 months later showed disappearance of the abnormal uptakes. With these facts, the major reason for the low uptake of ^{18}F -FSU-880 in his bone metastases seems to be the significantly decreased activity of the bone metastases induced by treatment, although reduction in lesion size by the treatment can also be a contributing factor. In case 4, multiple small but clear uptakes of ^{18}F -FSU-880 were observed in the bone, suggestive of small bone metastases. This suggests that small lesions can be detected if their activity is high enough and the increased uptake overcomes the negative effect of partial-volume effect.

In order to increase the detection rate of small lesions, increasing the lesion contrast is essential. Because the major route of excretion of ^{18}F -FSU-880 is from the kidney, sufficient hydration and/or the use of diuretics is expected to increase lesion contrast by facilitating the probe clearance from the body. In addition, in 5 out of 6 cases in the present study, the tumor uptake and image contrast of most lesions increased with time. Imaging at a later time point can further increase the image contrast and can improve the detection rate of small lesions, as reported for other PSMA-targeted probes.^{27,28}

The effect of treatment on the uptake of PSMA-targeted probe is not fully elucidated yet. Short-term androgen deprivation therapy has been reported to increase PSMA expression in castration-sensitive PC cells,²⁹ and long-term androgen deprivation therapy is reported to reduce the visibility of the lesions.³⁰ In the present patient cohort, cases 1 and 2 received PET/CT with no treatment. Cases 3, 4, and 6 were examined while undergoing treatment with enzalutamide or abiraterone acetate. Case 5 was during ^{223}Ra -chloride therapy. Except for case 5, in whom known lesions were not clearly visualized, known metastatic lesions were clearly visualized in the remaining 5 cases. As the number of patients was limited, it is not possible to elucidate the effect of treatment on probe uptake, and this remains to be verified in future studies. As for the

castration status of the present patients, case 2 can be regarded as castration-naïve at the time of ^{18}F -FSU-880 PET/CT, with the remaining 5 cases being castration-resistant. Except for case 5, whose metastases were inactive, metastatic lesions were clearly visualized in both castration-naïve and castration-resistant cases, and with this small patient population, it was not possible to conclude the effect of castration status on lesion uptake of ^{18}F -FSU-880. In terms of metastatic site, 5 cases had bone metastases and 1 case had LN metastasis. We did not experience visceral metastases such as liver or lung. With regard to the relatively high uptake of ^{18}F -FSU-880 in the liver, the detectability of hepatic metastases should be evaluated in the future.

With the increasing number of patients examined with PSMA-targeted probes, many pitfalls are emerging.³¹ In this study, we experienced abnormal uptakes in addition to known metastases in 3 cases. Although we did not try to confirm these additional uptakes as true positive or false positive in the present study, from the site of uptakes (prostate, bone, and pelvic LN) and follow-up image findings (bone metastases became evident in the follow-up bone scintigraphy in case 4, and decrease in the size of LN after treatment in case 2), these abnormal uptakes are more likely to be recurrent/metastatic lesions rather than false-positive uptakes. Otherwise, we

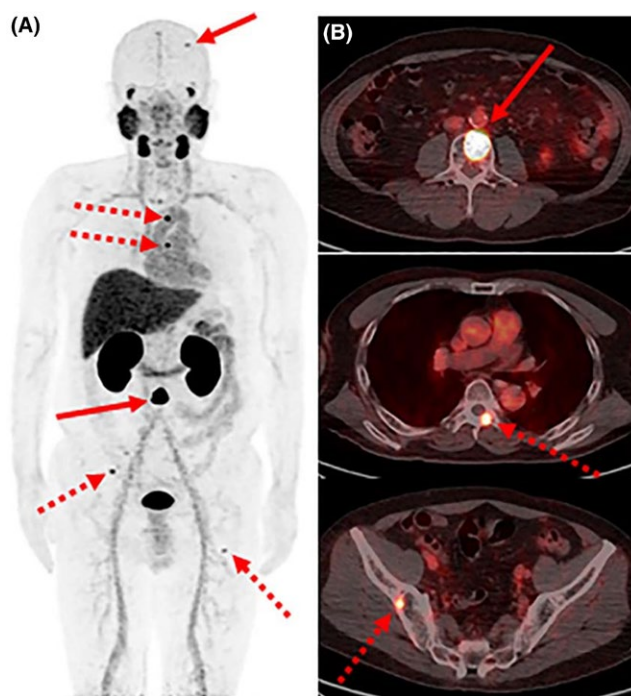


FIGURE 4 ^{18}F -FSU-880 PET/computed tomography (CT) images of case 4, a prostate cancer patient with known metastatic lesions, obtained 2 h after administration. In addition to the increased uptakes of ^{18}F -FSU-880 in the known bone metastases (arrows), small but clear uptakes were additionally observed in the bone, which were suggestive of small bone metastases (dotted arrows). A, Maximum intensity projection image. B, Transaxial positron PET/CT fusion images of known bone metastases and suspected small bone metastases

did not experience any false-positive uptakes such as inflammatory lesions or ganglia.

At present, ^{68}Ga -labeled probes targeting PSMA are most popular, especially ^{68}Ga -PSMA-11 (^{68}Ga -PSMA-HEBD-CC). ^{18}F -FSU-880 shares the same binding moiety with ^{68}Ga -PSMA-11, an asymmetric urea compound. In addition, ^{18}F -FSU-880 was designed to have an aromatic ring and succinimidyl moiety that are thought to be associated with high binding affinity. Direct comparison of the binding affinity indicated that ^{18}F -FSU-880 showed higher binding affinity than ^{18}F -DCFPyL.¹⁹ Although the binding affinity of ^{18}F -FSU-880 was not directly compared with that of ^{68}Ga -PSMA-11, it is reported that IC_{50} values determined by the competitive binding assay using LNCaP cells for ^{68}Ga -PSMA-11 and ^{18}F -DCFPyL were 24.3 and 22.8 nmol/L, respectively.^{32,33} Although these values should be cautiously compared, as the evaluation method was not exactly identical, ^{18}F -DCFPyL could have almost identical binding affinity to ^{68}Ga -PSMA-11. ^{18}F -FSU-880, therefore, is expected to have identical or even higher binding affinity than ^{68}Ga -PSMA-11. As for the tissue distribution, the physiological uptake pattern of ^{18}F -FSU-880 observed in the present study was almost identical to that of ^{68}Ga -PSMA-11, which is reasonable as ^{18}F -FSU-880 shares the same binding moiety as ^{68}Ga -PSMA-11. Dietlein et al compared the performance of ^{18}F - and ^{68}Ga -PSMA PET in patients with biochemical recurrence and concluded that ^{18}F -DCFPyL was non-inferior to ^{68}Ga -PSMA-11.²⁶ This suggests that ^{18}F -FSU-880 PET/CT can be as accurate as ^{68}Ga -PSMA-11 PET/CT in the detection of recurrent foci, which should be validated in future clinical studies.

In conclusion, the present first-in-man study confirmed that PET/CT with ^{18}F -FSU-880 can be safely carried out and could detect active metastatic lesions with high image contrast. The present results warrant further studies with a larger number of cases to verify the clinical utility of ^{18}F -FSU-880 PET/CT in the management of prostate cancer patients.

ACKNOWLEDGMENTS

This study was supported by the "Practical Research for Innovative Cancer Control" research grant (17ck0106149h003/18ck0106426 h001) from the Japan Agency for Medical Research and Development (AMED).

CONFLICT OF INTEREST

Hideo Saji and Hiroyuki Kimura of Kyoto University are holding a Japanese patent related to ^{18}F -FSU-880 (P6292568) along with Nihon Medi-Physics Co., Ltd. Tsuneo Saga is the endowed chair of the sponsored-research program by Nihon Medi-Physics Co., Ltd. Masahiro Ono, Hideo Saji, and Kaori Togashi receive research funding from Nihon Medi-Physics Co., Ltd.

ORCID

Tsuneo Saga  <https://orcid.org/0000-0001-7801-9316>

REFERENCES

- Attard G, Parker C, Eeles RA, et al. Prostate cancer. *Lancet*. 2016;387:70-82.
- National Cancer Center, Japan. Projected Cancer Statistics; 2017. https://ganjoho.jp/en/public/statistics/short_pred.html. Accessed October 27, 2017.
- Mohler JL, Armstrong AJ, Bahnson RR, et al. Prostate cancer, version 1.2016. *J Natl Compr Canc Netw*. 2016;14:19-30.
- Mottet N, Bellmunt J, Bolla M, et al. EAU-ESTRO-SIOG guidelines on prostate cancer. Part 1: Screening, diagnosis, and local treatment with curative intent. *Eur Urol*. 2017;71:618-629.
- Bouchelouche K, Turkbey B, Choyke PL. PSMA PET and radionuclide therapy in prostate cancer. *Semin Nucl Med*. 2016;46:522-535.
- Pinto JT, Suffoletto BP, Berzin TM, et al. Prostate-specific membrane antigen: a novel folate hydrolase in human prostatic carcinoma cells. *Clin Cancer Res*. 1996;2:1445-1451.
- Perner S, Hofer MD, Kim R, et al. Prostate-specific membrane antigen expression as a predictor of prostate cancer progression. *Hum Pathol*. 2007;38:696-701.
- Wright GL Jr, Haley C, Beckett ML, Schellhammer PF. Expression of prostate-specific membrane antigen in normal, benign, and malignant prostate tissues. *Urol Oncol*. 1995;1:18-28.
- Ross JS, Sheehan CE, Fisher HA, et al. Correlation of primary tumor prostate-specific membrane antigen expression with disease recurrence in prostate cancer. *Clin Cancer Res*. 2003;9:6357-6362.
- Silver DA, Pellicer I, Fair WR, Heston WD, Cordon-Cardo C. Prostate-specific membrane antigen expression in normal and malignant human tissues. *Clin Cancer Res*. 1997;3:81-85.
- Holmes EH. PSMA specific antibodies and their diagnostic and therapeutic use. *Expert Opin Investig Drugs*. 2001;10:511-519.
- Virgolini I, Decristoforo C, Haug A, Fanti S, Uprimny C. Current status of theranostics in prostate cancer. *Eur J Nucl Med Mol Imaging*. 2018;45:471-495.
- Lenzo NP, Meyrick D, Turner JH. Review of Gallium-68 PSMA PET/CT imaging in the management of prostate cancer. *Diagnostics*. 2018;8:16.
- Afshar-Oromieh A, Holland-Letz T, Giesel FL, et al. Diagnostic performance of ^{68}Ga -PSMA-11 (HBED-CC) PET/CT in patients with recurrent prostate cancer: evaluation in 1007 patients. *Eur J Nucl Med Mol Imaging*. 2017;44:1258-1268.
- Szabo Z, Mena E, Rowe SP, et al. Initial evaluation of [^{18}F]DCFPyL for prostate-specific membrane antigen (PSMA)-targeted PET imaging of prostate cancer. *Mol Imaging Biol*. 2015;17:565-574.
- Giesel FL, Hadaschik B, Cardinale J, et al. F-18 labelled PSMA-1007: biodistribution, radiation dosimetry and histopathological validation of tumor lesions in prostate cancer patients. *Eur J Nucl Med Mol Imaging*. 2017;44:678-688.
- von Eyben FE, Roviello G, Kiljunen T, et al. Third-line treatment and ^{177}Lu -PSMA radioligand therapy of metastatic castration-resistant prostate cancer: a systematic review. *Eur J Nucl Med Mol Imaging*. 2018;45:496-508.
- Kratochwil C, Bruchertseifer F, Giesel FL, et al. ^{225}Ac -PSMA-617 for PSMA-targeted α -radiation therapy of metastatic castration-resistant prostate cancer. *J Nucl Med*. 2016;57:1941-1944.
- Harada N, Kimura H, Onoe S, et al. Synthesis and biologic evaluation of novel ^{18}F -labeled probes targeting prostate-specific membrane antigen for PET of prostate cancer. *J Nucl Med*. 2016;57:1978-1984.
- Harada N, Kimura H, Ono M, Saji H. Preparation of asymmetric urea derivatives that target prostate-specific membrane antigen for SPECT imaging. *J Med Chem*. 2013;56:7890-7901.

21. Pfob CH, Ziegler S, Graner FP, et al. Biodistribution and radiation dosimetry of ^{68}Ga -PSMA HBED CC-a PSMA specific probe for PET imaging of prostate cancer. *Eur J Nucl Med Mol Imaging*. 2016;43:1962-1970.
22. The human protein atlas. FOLH1. Version: 18.1. <http://www.proteinatlas.org/ENSG00000086205/normal>. Accessed November 15, 2018.
23. Tagawa ST, Milowsky ML, Morris M, et al. Phase II study in lutetium-177-labeled anti-prostate-specific membrane antigen monoclonal antibody J591 for metastatic castration-resistant prostate cancer. *Clin Cancer Res*. 2013;19:5182-5191.
24. Taïeb D, Foletti JM, Bardès M, Rocchi P, Hicks RD, Haberkorn U. PSMA-targeted radionuclide therapy and salivary gland toxicity: why does it matter? *J Nucl Med*. 2018;59:747-748.
25. Cho SY, Gage KL, Mease RC, et al. Biodistribution, tumor detection, and radiation dosimetry of ^{18}F -DCFBC, a low-molecular-weight inhibitor of prostate-specific membrane antigen, in patients with metastatic prostate cancer. *J Nucl Med*. 2012;53:1883-1891.
26. Dietlein F, Kobe C, Neubauer S, et al. PSA-stratified performance of ^{18}F - and ^{68}Ga -PSMA PET in patients with biochemical recurrence of prostate cancer. *J Nucl Med*. 2017;58:947-952.
27. Afshar-Oromieh A, Sattler LP, Mier W, et al. The clinical impact of additional late PET/CT imaging with ^{68}Ga -PSMA-11 (HBED-CC) in the diagnosis of prostate cancer. *J Nucl Med*. 2017;58:750-755.
28. Rahbar K, Afshar-Oromieh A, Bögemann M, et al. ^{18}F -PSMA-1007 PET/CT at 60 and 120 minutes in patients with prostate cancer: biodistribution, tumour detection and activity kinetics. *Eur J Nucl Med Mol Imaging*. 2018;45:1329-1334.
29. Meller B, Bremmer F, Sahlmann CO, et al. Alterations in androgen deprivation enhanced prostate-specific membrane antigen (PSMA) expression in prostate cancer cells as a target for diagnostics and therapy. *EJNMMI Res*. 2015;5:66.
30. Afshar-Oromieh A, Debus N, Uhrig M, et al. Impact of long-term androgen deprivation therapy on PSMA ligand PET/CT in patients with castration-sensitive prostate cancer. *Eur J Nucl Med Mol Imaging*. 2018;45:2025-2054.
31. Hofman MS, Hicks RJ, Maurer T, Eiber M. Prostate-specific membrane antigen PET: clinical utility in prostate cancer, normal patterns, pearls, and pitfalls. *Radiographics*. 2018;38:200-217.
32. Wüstemann T, Bauder-Wüst U, Schäfer M, et al. Design of internalizing PSMA-specific Glu-ureido-based radiotherapeutics. *Theranostics*. 2016;6:1085-1109.
33. Kelly J, Amor-Coarasa A, Nikolopoulou A, et al. Synthesis and pre-clinical evaluation of a new class of high-affinity ^{18}F -labeled PSMA ligands for detection of prostate cancer by PET. *Eur J Nucl Med Mol Imaging*. 2017;44:647-661.

How to cite this article: Saga T, Nakamoto Y, Ishimori T, et al. Initial evaluation of PET/CT with ^{18}F -FSU-880 targeting prostate-specific membrane antigen in prostate cancer patients. *Cancer Sci*. 2019;110:742-750. <https://doi.org/10.1111/cas.13911>